

Interannual variability in associations between seasonal climate, weather, and extremes: wintertime temperature over the Southwestern United States

This content has been downloaded from IOPscience. Please scroll down to see the full text.

2015 Environ. Res. Lett. 10 124023

(<http://iopscience.iop.org/1748-9326/10/12/124023>)

View [the table of contents for this issue](#), or go to the [journal homepage](#) for more

Download details:

IP Address: 210.77.64.109

This content was downloaded on 17/04/2017 at 05:42

Please note that [terms and conditions apply](#).

You may also be interested in:

[Did European temperatures in 1540 exceed present-day records?](#)

Rene Orth, Martha M Vogel, Jürg Luterbacher et al.

[Persistent cold air outbreaks over North America in a warming climate](#)

Yang Gao, L Ruby Leung, Jian Lu et al.

[Impacts of climate extremes on gross primary production under global warming](#)

I N Williams, M S Torn, W J Riley et al.

[Observed connections of Arctic stratospheric ozone extremes to Northern Hemisphere surface climate](#)

Diane J Ivy, Susan Solomon, Natalia Calvo et al.

[How much global burned area can be forecast on seasonal time scales using sea surface temperatures?](#)

Yang Chen, Douglas C Morton, Niels Andela et al.

[Was the extreme Northern Hemisphere greening in 2015 predictable?](#)

Ana Bastos, Philippe Ciais, Taejin Park et al.

[Controls on interannual variability in lightning-caused fire activity in the western US](#)

John T Abatzoglou, Crystal A Kolden, Jennifer K Balch et al.

[Summertime atmosphere–ocean preconditionings for the Bering Sea ice retreat and the following severe winters in North America](#)

Takuya Nakanowatari, Jun Inoue, Kazutoshi Sato et al.

[Benchmarking carbon fluxes of the ISIMIP2a biome models](#)

Jinfeng Chang, Philippe Ciais, Xuhui Wang et al.

Environmental Research Letters



LETTER

Interannual variability in associations between seasonal climate, weather, and extremes: wintertime temperature over the Southwestern United States

OPEN ACCESS

RECEIVED
2 September 2015REVISED
23 November 2015ACCEPTED FOR PUBLICATION
25 November 2015PUBLISHED
22 December 2015

Content from this work may be used under the terms of the [Creative Commons Attribution 3.0 licence](#).

Any further distribution of this work must maintain attribution to the author(s) and the title of the work, journal citation and DOI.



Kristen Guirguis, Alexander Gershunov and Daniel R Cayan

Scripps Institution of Oceanography, La Jolla, CA, USA

E-mail: kguirguis@ucsd.edu**Keywords:** winter temperature extremes, Southwest United States, temperature probability distribution functions, natural climate variabilitySupplementary material for this article is available [online](#)**Abstract**

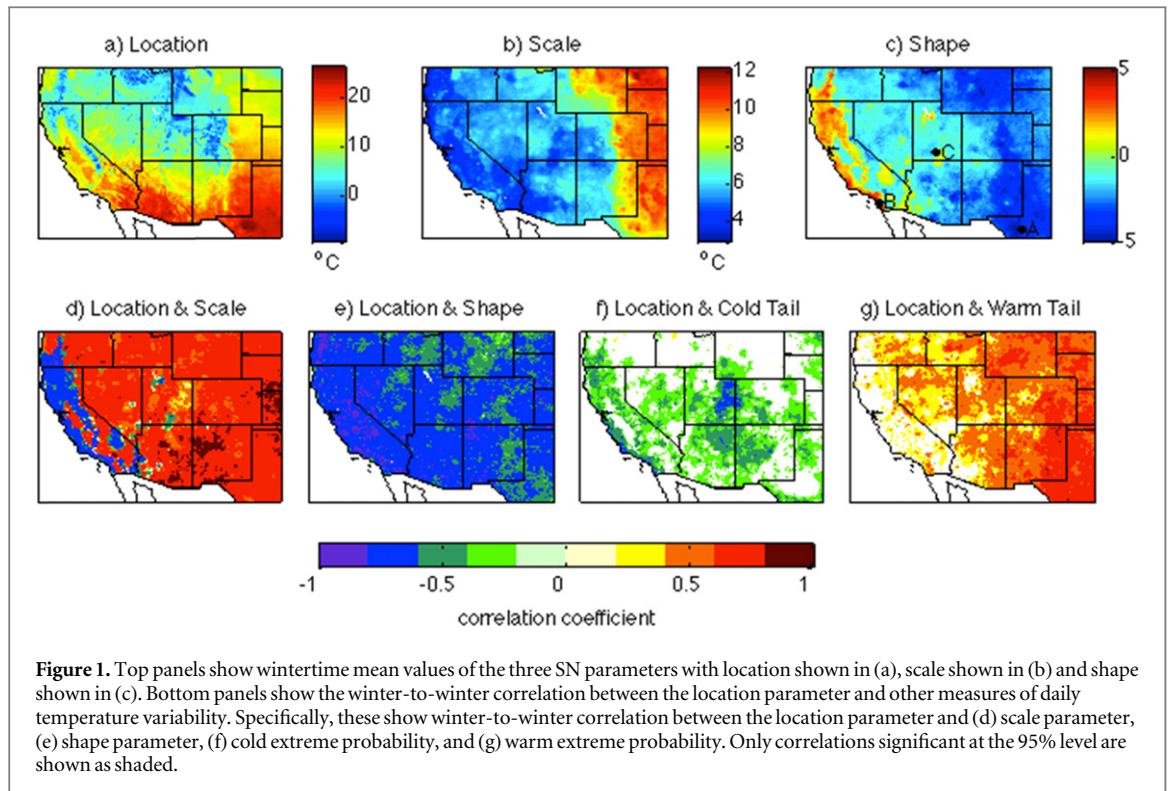
Temperature variability in the Southwest US is investigated using skew-normal probability distribution functions (SN PDFs) fitted to observed wintertime daily maximum temperature records. These PDFs vary significantly between years, with important geographical differences in the relationship between the central tendency and tails, revealing differing linkages between weather and climate. The warmest and coldest extremes do not necessarily follow the distribution center. In some regions one tail of the distribution shows more variability than does the other. For example, in California the cold tail is more variable while the warm tail remains relatively stable, so warm years are associated with fewer cold extremes but not necessarily more warm extremes. The opposite relationship is seen in the Great Plains. Changes in temperature PDFs are conditioned by different phases of El Niño-La Niña (ENSO) and the Pacific decadal oscillation (PDO). In the Southern Great Plains, La Niña and/or negative PDO are associated with generally warmer conditions. However, in terms of extremes, while the warm tails become thicker and longer, the cool tails are not impacted—extremely warm days become more frequent but extremely cool days are not less frequent. In contrast, in coastal California, La Niña or negative PDO bring generally cooler conditions with more/stronger cold extremes but the warm extreme probability is not significantly affected. These results could have implications for global warming. If a rigid shift of the whole range occurs, then warm years are not necessarily a good analogue for a warmer climate. If global warming instead brings regional changes more aligned with a preferred state of dominant climate variability modes, then we may see asymmetric changes in the tails of local temperature PDFs.

1. Introduction

The seasonal climate of each sub-region in a geographically complex domain, such as the Southwestern United States, reflects the interaction of several weather patterns impacting a given locality. For example, winter in southern coastal California is marked by an interplay of onshore (westerly humid maritime) and offshore (easterly dry warm continental-desert) flow (Conil and Hall 2006) punctuated now and then by frontal precipitation associated with midlatitude cyclones and cold outbursts associated

with northerly along-shore flow around transient anticyclones (Favre and Gershunov 2006, 2009). Along Colorado's front range, as another example, winter climate is marked by cold outbreaks associated with surface anticyclones, *Northers*, steered southward by the front range of the Rockies and warm bursts due to downslope foehn-type winds known as *Chinooks*.

Each locality gets weather patterns that define its climate, and local climate variability is driven by their relative frequency, duration and intensity. A particular winter's anomalous climate is defined by the relative absence or presence of characteristic weather features.



Some of these patterns are benign, others, especially if extreme and occurring when the environment is appropriately primed, can have major impacts on society including sectors such as health, energy, agriculture, and transportation.

Realizing that seasonal mean climate is influenced by extreme weather and that extreme weather statistics can sometimes be more seasonably predictable than mean climate (Gershunov 1998), we adapt a parametric framework to summarize the relationships between local daily weather and seasonal climate. In practice, the mean has been the orthodox measure of central tendency to define an anomalously warm or cold season. However, the mean best reflects central tendency when the distribution is symmetric (e.g. normal). In reality, seasonal distributions of daily temperature are not typically symmetric climatologically (Cavanaugh and Shen 2014) and anomalous seasons can be characterized by changes in variance or skew as well as changes in central tendency. In skewed distributions particularly, extremes and outliers unduly influence the mean. Therefore, a parametric framework to quantify the shape of the seasonal distribution and provide a comprehensive perspective on anomalous seasons in a variable climate is needed. In particular, we aim to reveal relationships between seasonal climate and daily weather over space and time.

Simolo *et al* (2010) fit skew-normal probability density functions (SN PDFs) to study seasonal trends in daily temperature over Italy. Below, we fit SN PDFs to maximum daily temperatures (T_{max}) in winter, resolving the Southwestern US on a 6 km grid, and examine how the weather–climate relationships

evolve from year-to-year over a data record spanning 62 winters. This methodology aims to quantify local weather–climate relationships as the climate varies from winter-to-winter over the Southwest.

In what follows, we describe the data and methodology; examine the climate-scale variability in local weather–climate relationships; quantify the effects of the two dominant modes of regional climate variability, which are the known natural sources of climate predictability, on these relationships in the Southwest; and conclude with a view towards future climate research and societal implications.

2. Data

We use daily maximum temperature data from Livneh *et al* (2013), which is an observationally-based gridded product derived from daily station data interpolated to a $1/16^\circ$ latitude–longitude grid. The source data are the cooperative observer (coop) summaries of the day from the National Climatic Data Center (NCDC) supplemented by first-order automated surface observing system observations (National Climatic Data Center 2009). The Livneh product is an update/extension of the extensively used product of Maurer *et al* (2002), where updates include higher spatial resolution and extended period of analysis. For this study we analyze the full temperature distribution for 62 DJF winter seasons from December 1949 through February 2011 over the Southwest US (west of 100°W and south of 45°N). As a verification measure, we compared the gridded product with station

observations at three locations near those shown in figure 1(c). The year-to-year variability of the first three statistical moments (mean, variance, and skewness) is represented extremely well by the gridded product (correlation >0.97 in all comparisons). We chose maximum temperatures in winter because (1) winter has the strongest day-to-day weather variability (not shown) and most predictable climate variations (Gershunov and Cayan 2003) of any season and (2) the Southwest has seen less recent warming in wintertime maximum temperatures, compared to other seasons (Hoerling *et al* 2013) and compared to minimum temperatures, thus allowing a sharper and more stationary examination of natural climate variability.

3. Skew-normal (SN) methodology and southwestern climatology

Daily wintertime temperature distributions over the Southwest are not symmetric. They exhibit various degrees and directions of skewness, which are not represented by the traditional Gaussian (i.e. normal) distribution (figure S1). Coastal California and the Sierra Nevada and Cascade mountains exhibit positive skew while over the rest of the Southwest negative skew is observed. Even locations where distributions appear normal climatologically may exhibit varying degrees of seasonal skew from year-to-year. To account for skewness and identify changes in the shape of the temperature PDF due to interannual variability, we model observations using the SN PDF. The SN was developed as an extension of the Gaussian by including a shape parameter to allow for asymmetry, and where the Gaussian is a special case of the SN when the shape parameter is zero (Azzalini 2005). Therefore, the SN offers more flexibility in fitting skewed data and we find it particularly useful for analyzing varying climatic structure reflected in space-time PDF shape differences. The SN is appropriate for a variable characterized by two exponentially-decaying probability tails reflecting extreme behavior on either side, e.g. seasonal PDFs of daily temperature, which can be normal or positively or negatively skewed depending on geographic location or year. The SN distribution is represented by three parameters: location, scale and shape. Location is a measure of central tendency, scale is a measure of dispersion about the central tendency, and shape is a measure of skew. They are closely related to but not equal to the three first moments: mean, variance, and skewness, respectively. The correlation between the location parameter and the mean is 0.52 on average over the Southwest, which reflects the year-to-year changes in the shape of the pdf. The mean will be warmer (colder) than the location parameter in years that are more positively (negatively) skewed because the mean is heavily influenced by extremes

and outliers. A stronger correlation is observed between the scale parameter and variance ($r = 0.77$) and between the shape parameter and skewness ($r = 0.68$).

The location parameter is most closely related to the mode of the distribution and is a much better estimate of central tendency in skewed distributions than is the mean, which is pulled in the direction of the longer tail. In our analyses and discussion we define warm and cold years by central tendency as estimated by the location parameter.

In our analysis, SN was found to be superior to Gaussian at representing daily maximum temperatures (T_{max}) over the Southwest. We used the log likelihood ratio test (LLRT) applied to 62 winter seasons at each location. The LLRT is given by $D = -2 \ln(\text{likelihood of null model } (H_o) / \text{likelihood of alternative model } (H_a))$, where H_o is the Gaussian distribution and H_a is the SN. The null hypothesis representing the traditional Gaussian model was rejected in favor of SN at over 99% of the locations and winters. A demonstration of SN's ability to represent the temperature distribution at different locations in the Southwest is provided in figure S1 of the supplemental materials. The SN is shown capable of accurately representing the characteristic temperature distribution including high and low percentiles. In particular, the observed 90th and 10th percentiles are estimated extremely well by SN. One important benefit of the SN approach is the ability to estimate many different metrics from only three parameters. This would be highly useful for high-resolution climate change studies, for example, which requires downscaled analyses from multiple models and scenarios. Although here we focus only on the 10th and 90th percentile, we could obtain from only three parameters many applied metrics such as heating or cooling degree-days, freeze days, or probability of exceeding any quantile or threshold value.

Figures 1(a)–(c) display mean values of the three SN parameters over the Southwest, showing climatologically most frequent warm winter temperatures (i.e. warmest winters) clustered around the southern part of the domain, as indicated by the location parameter (figure 1(a)) while the largest variance is observed along the eastern edge of the region on the lee side (the Front Range) of the Rockies (scale parameter, figure 1(b)). The shape parameter shown in figure 1(c) clearly shows that temperature distributions are skewed in the Southwest, with most locations exhibiting negative skew, i.e. a proclivity for cold extremes relative to central tendency. The greatest negative skew occurs along the Front Range where transient anticyclones, the Northers, produce frequent cold snaps (Colle and Mass 1995). The exception is coastal California and parts of the Sierra and Cascade Ranges where a positively skewed distribution is observed. The greatest positive skew occurs in coastal southern

California where Santa Ana winds are common in winter. These katabatic winds originate from cold air masses in the elevated Great Basin, pushed coastward by synoptic pressure gradients, accelerating down-slope, heating adiabatically and drying on their way to sea level (Hughes and Hall 2010). The shape parameter appears sensitive to these regional weather patterns associated with local temperature extremes. For example, the warmest (coldest) 10% of days are about 7 °C warmer (1 °C colder) than the mode of the distribution in Oceanside, California (Point B shown in figure 1(c) and S1), while at Little Mexico, Texas (Point A), cold extremes tend to deviate more than three-fold from the mode compared to warm extremes (13 °C versus 4 °C).

4. Interannual variability and the temperature PDF

While the fitted SN parameters are independent in theory, we observe a strong empirical dependence among the local parameters, which reflects features of regional weather and climate over the Southwest. Figure 1(d) shows strong winter-to-winter correlation between the location and scale parameters showing that shifts in central tendency tend to be accompanied by changes in variance. In areas where temperatures are positively skewed (see figure 1(c)), such as the California coast and mountains, this relationship between location and scale is negative meaning that cool (warm) winters are accompanied by more (less) variance. Also in this region there is a negative correlation between location and shape (figure 1(e)), meaning that warmer winters are less positively skewed. We observe the opposite relationship in the rest of the domain where temperatures are negatively skewed. Here, cool (warm) winters are accompanied by less (more) variance. The correlation between the location and shape parameter is again negative, in this case meaning that warmer winters are more negatively skewed.

The relationship between the location parameter and the probability of occurrence of cold or warm extremes is shown in figures 1(f) and (g), where warm (cold) extreme probability is defined as the probability of exceeding (being colder than) the 90th (10th) percentile thresholds. For most of the domain (excepting California), a positive shift in the location parameter is associated with a higher probability of warm extremes (figure 1(g)), while the probability of a cold extreme is not well correlated with a shift in the location parameter (figure 1(f)). Therefore warmer winters in these parts come with a greater occurrence of warm extremes, but not necessarily with fewer cold extremes. In California, the opposite is true—cool winters associate with a higher probability of cold extremes but not necessarily with fewer warm extremes. The four-corners region shows a negative

(positive) relationship between the location parameter and cold (warm) extremes, so this region varies more symmetrically with warm winters being associated with more warm extremes and fewer cold extremes and cool winters with more cold extremes and fewer warm extremes.

To illustrate the interannual variability of daily temperatures throughout the Southwest, we performed a rotated principal component (RPC)-based regionalization using the methodology described in Gershunov and Guirguis (2012). By this methodology a grid cell is assigned to the RPC that best describes its temporal variability, and locations that are similarly assigned to the same RPC are grouped together into a 'region'. In this case, we aim to identify climate regions where the shape of the temperature PDF evolves (expands and contracts and leans) similarly across winter seasons. We applied this type of regionalization three times, once for each of the SN parameters, therefore each grid cell was assigned to a location region, a scale region, and a shape region. We then identified unique combinations of the three regional identifiers. This resulted in 139 distinct regions. However, we found that more than 75% of the spatial domain is represented by only eight major regions. Figure 2 shows the major climate regions along with the inter-annual behavior of the temperature PDF denoted by a representative grid cell within each region. Specifically the PDFs are shown for the ten warmest and coldest winters, where 'warmest' and 'coldest' are determined by the distribution center, as measured by the fitted location parameter.

In the four corners and extending south (e.g. Southern Great Plains, Madrean Sky Islands and Southern Colorado Plateau), cold winters are closer to Gaussian, while warm winters are strongly negatively skewed. Similar behavior is seen for the Northern Great Plains, Snake River Plateau and Basin and Range regions, although with a less dramatic shift or more variability in the cold winter PDF. For the California Coast and Mountains, the warm winter PDF is closer to Gaussian while cold winters show strong positive skew. Figure S2 shows the result of a t-test for unequal means applied to the tails of each PDF to determine whether the probability of warm or cold extremes is significantly different in warm versus cold winters. Here we see that for the four corners and inter-mountain regions (Basin and Range and Northern and Southern Colorado Plateau regions), the probabilities of both warm and cold extremes are related to shifts in central tendency (ttest is significant at the 95% level for both warm and cold extreme probabilities). For the California Coast and Mountains region, it is mainly the cold extreme probability that varies in a warm versus cold winter. To the north and east of the Rockies, it is primarily the warm tail of the PDF that is related to the central tendency.

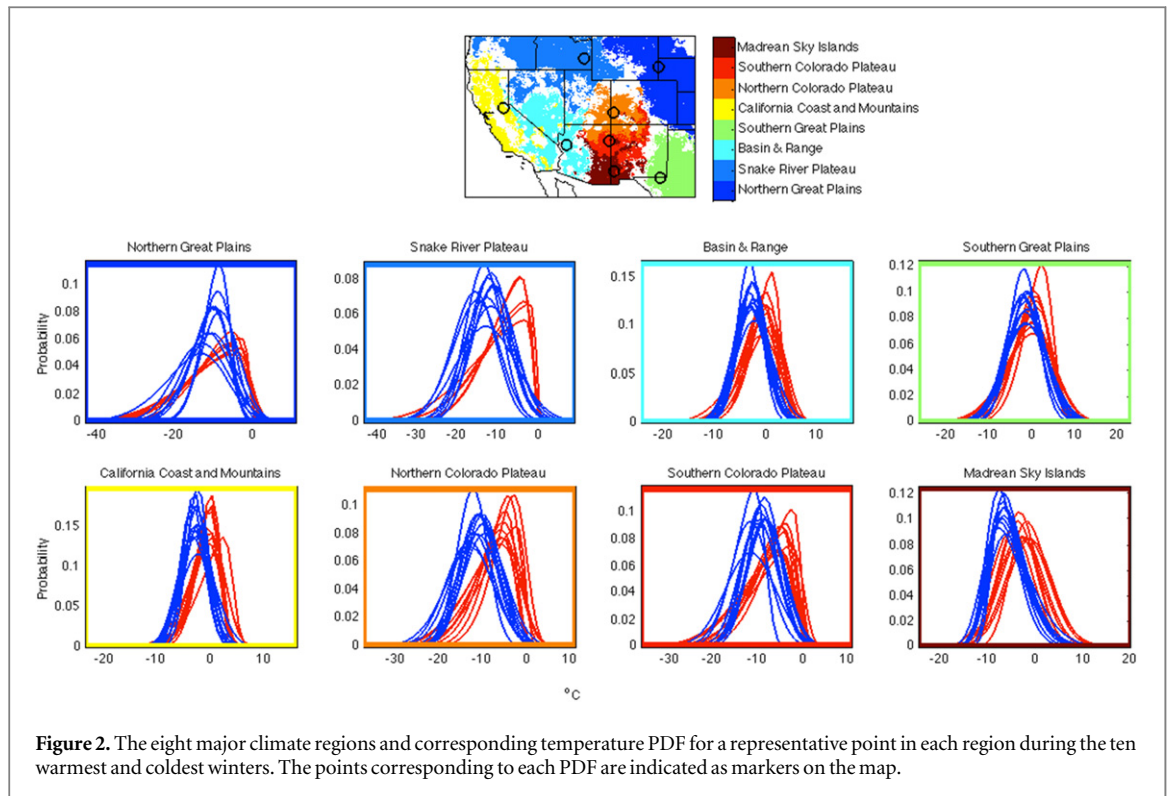


Figure 2. The eight major climate regions and corresponding temperature PDF for a representative point in each region during the ten warmest and coldest winters. The points corresponding to each PDF are indicated as markers on the map.

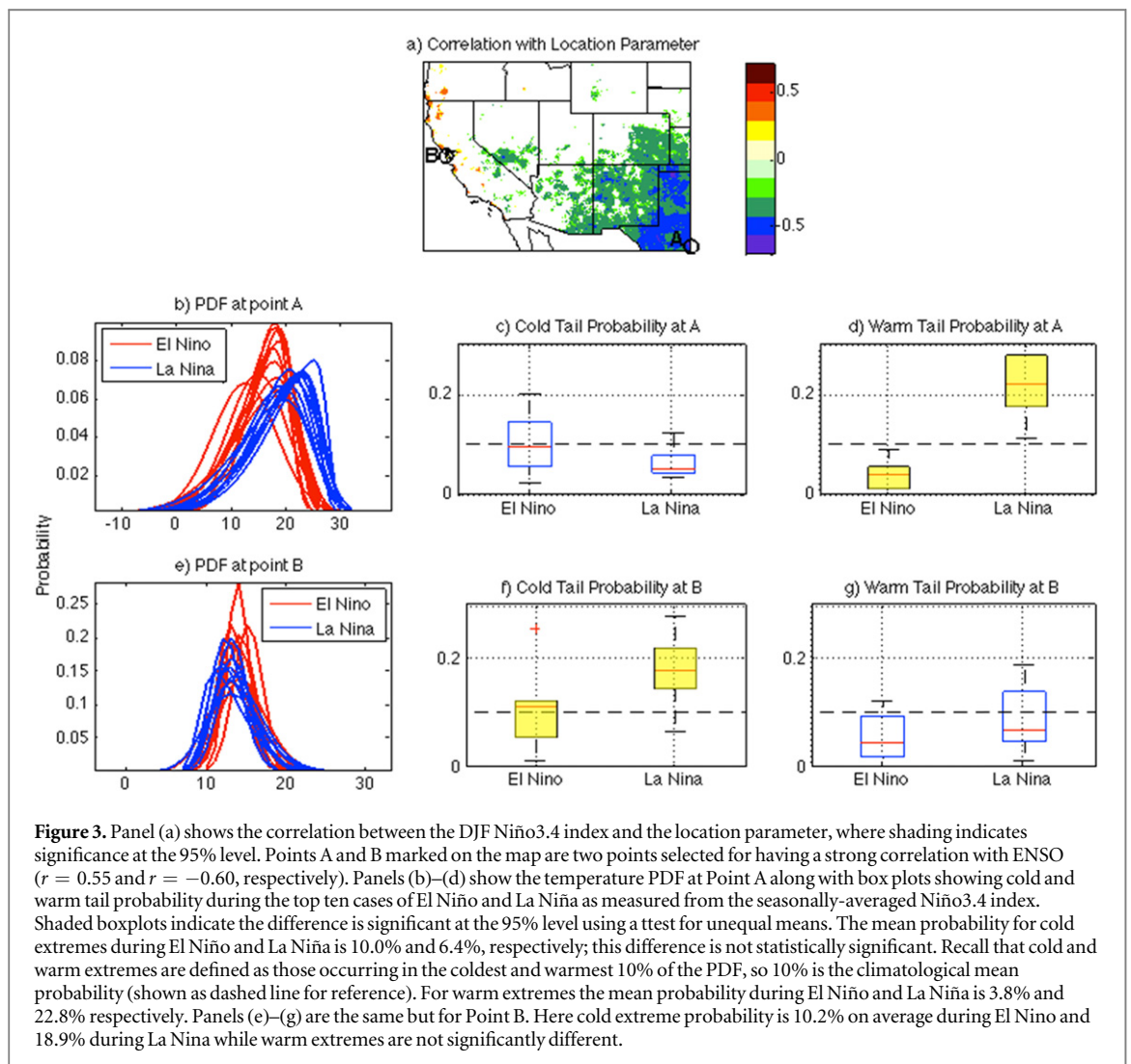
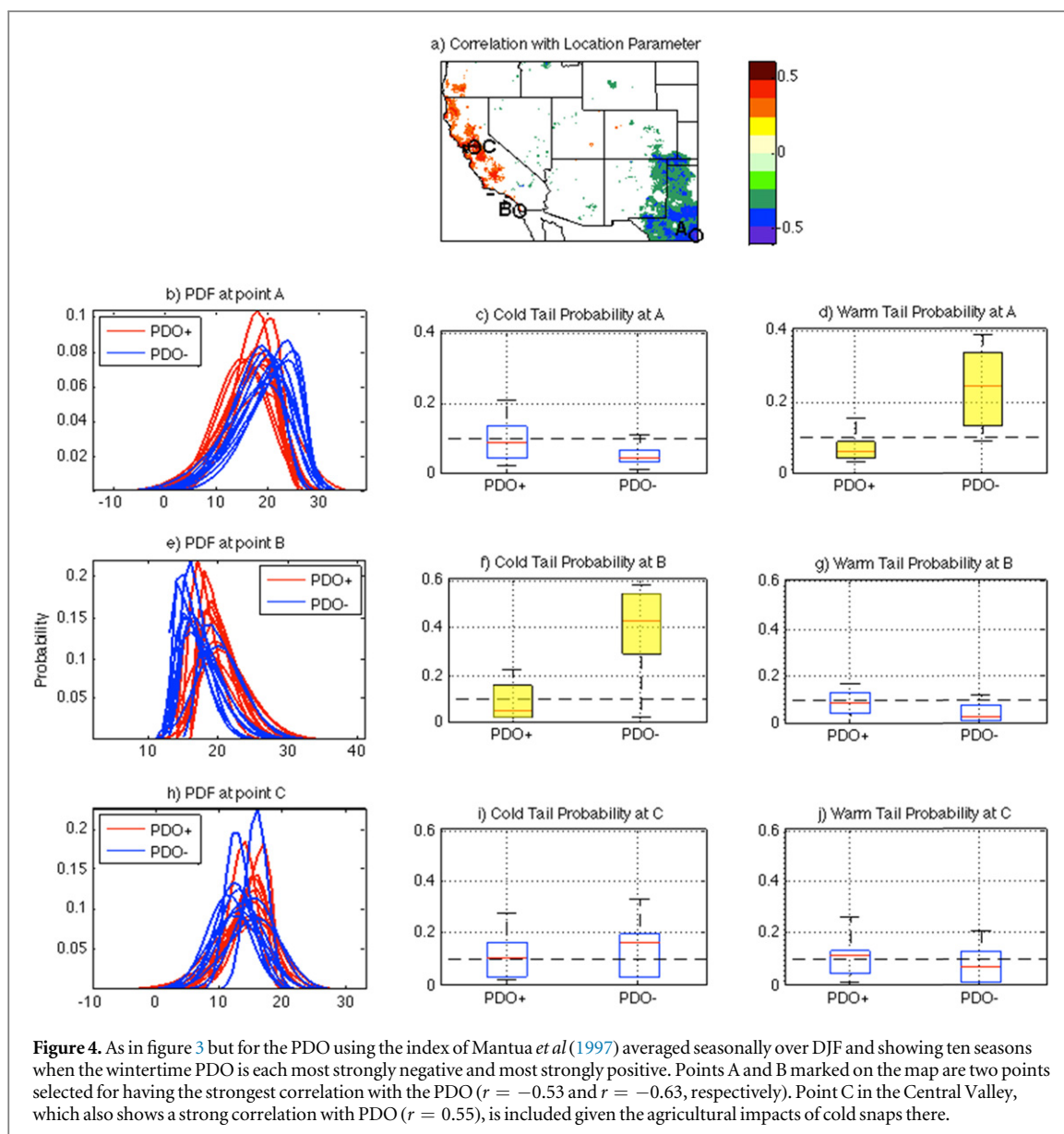


Figure 3. Panel (a) shows the correlation between the DJF Niño3.4 index and the location parameter, where shading indicates significance at the 95% level. Points A and B marked on the map are two points selected for having a strong correlation with ENSO ($r = 0.55$ and $r = -0.60$, respectively). Panels (b)–(d) show the temperature PDF at Point A along with box plots showing cold and warm tail probability during the top ten cases of El Niño and La Niña as measured from the seasonally-averaged Niño3.4 index. Shaded boxplots indicate the difference is significant at the 95% level using a test for unequal means. The mean probability for cold extremes during El Niño and La Niña is 10.0% and 6.4%, respectively; this difference is not statistically significant. Recall that cold and warm extremes are defined as those occurring in the coldest and warmest 10% of the PDF, so 10% is the climatological mean probability (shown as dashed line for reference). For warm extremes the mean probability during El Niño and La Niña is 3.8% and 22.8% respectively. Panels (e)–(g) are the same but for Point B. Here cold extreme probability is 10.2% on average during El Niño and 18.9% during La Niña while warm extremes are not significantly different.



5. ENSO and Pacific decadal oscillation (PDO)

Figure 3(a) shows the correlation between the NIÑO3.4 index and the location parameter. ENSO influence is observed most prominently in the Southern Great Plains region that includes Texas, New Mexico, and parts of Colorado and Arizona. This is part of a larger pattern of ENSO influence that is observed over the entire US Gulf Coast (not shown). Figures 3(b)–(d) show the temperature PDFs and cold and warm tail probabilities at a representative grid cell in the Southern Great Plains region. We see a greater and significant ENSO impact on warm extremes compared to cold ones. The mean probability of warm extremes during El Niño winters is less than half- while for La Niña it is more than twice the climatological expectation (3.8% and 22.8%, respectively).

Figure 3(a) also shows a significant ENSO relationship along the California coast, where El Niño (La

Niña) is associated with warmer (cooler) conditions. The probability of warm extremes is not significantly different during El Niño versus La Niña (figures 3(e)–(g)). Cold extreme probability is 10% (the climatological expectation) on average during El Niño and 19% during La Niña winters. This implies that El Niño exerts little influence over cold extremes while La Niña significantly increases their probability of occurrence along the California coast in winter, reflecting the fact that La Niña promotes high-amplitude anticyclonic circulation over the eastern North Pacific associated with frequent transient anticyclones reaching the California coast and stimulating cold air advection, as described by Favre and Gershunov (2006).

Since PDO has been shown to exert an even stronger influence on anticyclonic activity along the coast of California (Favre and Gershunov 2006), we examined PDO influences on temperature PDFs (figure 4). As with ENSO, PDO displays significant relationships with the location parameter in the Southern Great

Plains and coastal California, but now including the Central Valley (figure 4(a)). The Southern Great Plains (figures 4(b)–(d)) exhibit no significant change in cold tail probability but a strong PDO influence on warm tails is evident. Mean warm tail probability is three times higher under a strongly negative PDO (23.2%) than under a strongly positive PDO (7.4%). In coastal southern California (figures 4(e)–(g)) PDO primarily affects cold extremes. Here, cold tail probability ranges from an average of 0.81% for a strongly positive PDO to 36.9% under a strongly negative PDO. Because the distribution is strongly skewed (see figure 4(e)), a small shift in the location parameter ($\sim 2^\circ\text{C}$ in this case) results in a large change in cold tail probability ($\sim 36\%$ in this case).

While PDO influences the central tendency of the temperature PDF in the Central Valley (figure 4(a)), there is no influence seen for probability of extreme temperatures (figures 4(h)–(j)). This is consistent with the results of section 4 in which no significant relationship was found between the location parameter and warm or cold extremes in the Central Valley (see figures 1(f) and (g)).

6. Discussion and conclusions

We studied the variability of winter temperature over the Southwest US using a SN theoretical PDF fitted to daily maximum temperatures on a 6km grid for each year during a six and a half decades span. We tested and found the SN PDF to be superior to the Gaussian at representing temperature PDFs in the Southwest. The SN model was particularly effective at modeling year-to-year changes in the shape of the temperature PDF due to natural variability and it provided a framework for analyzing seasonal climate variability in a way that resolves daily weather. We analyzed the PDF parameters over space and time to investigate how changes in extreme weather events correspond to changes in the central tendency.

The relationship between the center and tails of the temperature distribution exhibits important geographical differences. In coastal California and mountains we find that cool (warm) winters are accompanied by more (less) variance. Here, a positive shift in the distribution center is associated with a lower probability of cold extremes but the probability of warm extremes does not vary with the central tendency. Furthermore, shifts in PDFs appear to be systematically modulated by ENSO and PDO. Along the California coast during La Niña or negative PDO, generally cooler conditions have occurred as expressed by cooler central tendencies and cold extremes; however warm extreme probability is not significantly affected by the cool phase of ENSO/PDO. The warm phase of ENSO/PDO exerts little influence over temperature extremes, warm or cold, in this region. In California Santa Ana winds are associated with coastal warm

extremes in winter, and these appear to be equally prevalent in warm and cold winters or different phases of ENSO/PDO as seen by the relative stability of the warm tail of the PDF. This stability of the warm tail relative to the cold tail explains the negative relationship observed between the location and scale and between location and shape in this region.

A nearly opposite pattern is found in the Great Plains and Snake River Plateau. In this region, cool winters are accompanied by less variance. Warmer winters exhibit greater variance, associated with more and stronger warm extremes but not with fewer cold extremes. The strongest ENSO/PDO influence is in the Southern Great Plains where La Niña and negative PDO are associated with generally warmer conditions. However, in terms of extremes, only the warm tails are impacted. So during La Niña or negative PDO, we identify warmer temperatures overall with more and stronger warm extremes but not necessarily fewer cold extremes.

These results suggest that in parts of the Southwest one tail of the distribution may be inherently more predictable than the other on seasonal timescales, perhaps even more than the central tendency. These climate–weather relationships are partly driven by ENSO and the PDO. For example, the warm and cold winters highlighted in figure 2 include positive, negative, and neutral phases of ENSO/PDO, so these climate forcings contribute to, but do not fully explain, the observed interannual variability. The results shown in figure 2 do not change appreciably when restricted to neutral phases of ENSO, for example.

Another question naturally arises: to what extent can fluctuations in climate be described by rigid PDF shifts rather than by changes in extreme events, wherein the tails of the PDF are distorted differently than the central tendency? The present study indicates that answering this question requires careful meteorological analyses for specific subregions. For example, we are not aware of existing work examining the climatic behavior of Northers responsible for cold extremes in the Great Plains. As another regional example, along the California coast and coastal valleys (including the agriculturally vital Central Valley), anticyclonic transients promoted by negative PDO and ENSO conditions cause cold extremes (Favre and Gershunov 2006). Negative PDO and ENSO phases are also predictably associated with less frequent and less intense rainfall (Gershunov and Barnett 1998, Gershunov and Cayan 2003). Why these conditions do not seem to significantly affect warm extremes typically associated with katabatic winds in coastal California winter is a topic of current research.

A related question is how temperature PDFs will vary under climate change. What will be the role of extreme events in driving future climate change and its impacts? Will observed relationships between the center and tails of the temperature distribution hold up? If so, then as mean temperatures rise, we might expect to

see a greater impact on warm extreme probability than on cold extreme probability in the Great Plains, and with the opposite outcome in California. Or possibly climate change will affect temperature distributions differently than we observe under natural variability if different mechanisms will be involved. We have reason to expect that some mechanisms will be similar as wintertime climate over the eastern north Pacific is expected to gradually become more anticyclonic (Favre and Gershunov 2009), e.g. more reminiscent of La Niña/PDO- conditions. As the stormtrack retreats poleward and precipitation frequency decreases (Polade *et al* 2014), will cold extremes relative to a new warmer baseline become more frequent in California?

Acknowledgments

This work was supported by DOI via the Southwest Climate Science Center on a grant titled: ‘Natural variability in the changing climate: Interaction of interannual, decadal, and century timescales with daily weather’, by the National Science Foundation via grant #F12078-2013-005, and by NOAA via the RISA program through the California and Nevada Applications Center. The temperature dataset is freely and publicly available from the University of Washington (<ftp://ftp.hydro.washington.edu/pub/blivneh/CONUS/>). We thank Mary Tyree for data retrieval and handling. We thank three anonymous reviewers for helpful comments during the evaluation of this paper.

References

- Azzalini A 2005 The skew-normal distribution and related multivariate families *Scand. J. Stat.* **32** 159–88
- Cavanaugh N R and Shen S S P 2014 Northern Hemisphere climatology and trends of statistical moments documented from GHCN-daily surface air temperature station data from 1950 to 2010 *J. Clim.* **27** 5396–410
- Colle B A and Mass C F 1995 The structure and evolution of cold surges east of the rocky mountains *Mon. Weather Rev.* **123** 2577–610
- Conil S and Hall A 2006 Local regimes of atmospheric variability: a case study of southern California *J. Clim.* **19** 4308–25
- Favre A and Gershunov A 2006 Extra-tropical cyclonic/anticyclonic activity in North-Eastern Pacific and air temperature extremes in Western North America *Clim. Dyn.* **26** 617–29
- Favre A and Gershunov A 2009 North Pacific cyclonic and anticyclonic transients in a global warming context: possible consequences for Western North American daily precipitation and temperature extremes *Clim. Dyn.* **32** 969–87
- Gershunov A 1998 ENSO influence on intraseasonal extreme rainfall and temperature frequencies in the contiguous US: implications for long-range predictability *J. Clim.* **11** 3192–203
- Gershunov A and Barnett T 1998 Inter-decadal modulation of ENSO teleconnections *Bull. Am. Meteorol. Soc.* **79** 2715–25
- Gershunov A and Cayan D 2003 Heavy daily precipitation frequency over the contiguous United States: sources of climatic variability and seasonal predictability *J. Clim.* **16** 2752–65
- Gershunov A and Guirguis K 2012 California heat waves in the present and future *Geophys. Res. Lett.* **39** L18710
- Hoerling M P, Dettinger M, Wolter K, Lukas J, Eischeid J, Nemani R, Liebmann B and Kunkel K E 2013 Present weather and climate: evolving conditions *Assessment of Climate Change in the Southwest United States: A Report Prepared for the National Climate Assessment* a report by the Southwest Climate Alliance ed G Garfin *et al* (Washington, DC: Island Press) pp 74–100
- Hughes M and Hall A 2010 Local and synoptic mechanisms causing Southern California’s Santa Ana winds *Clim. Dyn.* **34** 847–57
- Livneh B, Rosenberg E A, Lin C, Nijssen B, Mishra V, Andreadis K M, Maurer E P and Lettenmaier D P 2013 A long-term hydrologically based dataset of land surface fluxes and states for the conterminous United States: update and extensions *J. Clim.* **26** 9384–92
- Mantua N J, Hare S R, Zhang Y, Wallace J M and Francis R C 1997 A Pacific interdecadal climate oscillation with impacts on salmon production *Bull. Am. Meteorol. Soc.* **78** 1069–79
- Maurer E P, Wood A W, Adam J C, Lettenmaier D P and Nijssen B 2002 A long-term hydrologically-based data set of land surface fluxes and states for the conterminous United States *J. Clim.* **15** 3237–51
- National Climatic Data Center 2009 *Data Documentation for Data Set 3200 (DSI-3200): Surface Land Daily Cooperative Summary of the Day, Report* Asheville, NC (www1.ncdc.noaa.gov/pub/data/documentlibrary/tddoc/td3200.pdf)
- Polade S D, Pierce D W, Cayan D R, Gershunov A and Dettinger M D 2014 The key role of dry days in changing regional climate and precipitation regimes *Nat. Sci. Rep.* **4** 4364
- Simolo C, Brunetti M, Maugeri M, Nanni T and Speranza A 2010 Understanding climate change—induced variations in daily temperature distributions over Italy *J. Geophys. Res.* **115** D22110